Monolithic Fused Silica Fiber Attachment Ears for Larger Test Masses in Third-Generation Gravitational Wave Detectors

Emma Bollinger[1]

Advised by Dr. A.V. Cumming[2] and Prof. Giles Hammond[2]

[1] *Departments of Mathematics and Engineering Physics, Southwestern Oklahoma State University, Weatherford, OK, USA*
[2] *Institute for Gravitational Research, Department of Physics and Astronomy, SUPA University of Glasgow, Glasgow, UK*

This paper explores possible adjustments to the silica "ears" that are an essential piece of the monolithic stages of LIGO's quadruple suspensions. We look at how changing different parameters affects stress distributions in the ears, and propose redesigns to implement in larger ears for the 05+ upgrade to advanced LIGO. We attempt to meet new design criteria without letting maximum stress in the ear deviate far from the current 12.4 MPa.

I. INTRODUCTION

Gravitational waves are ripples in the curvature of space-time that propagate from super-energetic cosmic events such as the collision of two black holes. Gravitational waves were first successfully observed in 2015 by the advanced Laser Interferometer Gravitational-Wave Observatory (aLIGO) collaboration[11]. The optics involved in LIGO's interferometer are each isolated on a four-stage quadruple suspension, the last two stages of which are of interest to this project. Detection of low-frequency (10-30 Hz) [2] events requires ultra-low levels of noise in the final suspension stage (in which the optic, or "test mass", is held). Thermal displacement noise, $x(\omega)$, is calculated using the following fluctuation-dissipation theorem:

$$x(\omega) = \sqrt{\frac{4k_BT}{m\omega}\left(\frac{{\omega_0}^2\Phi(\omega)}{{\omega_0}^4\Phi^2(\omega) + ({\omega_0}^2 - \omega^2)^2}\right)}$$

where T= temperature, m= pendulum mass, $\Phi(\omega)$= pendulum mode's mechanical loss angle, ω_0= resonant angular frequency, k_B= Boltzmann's Constant, and ω= angular frequency of interest.[13, 10]

Fused silica is the material of choice for the monolithic final stage of the suspension[5]. It has very low mechanical loss[9] (internal mechanical energy dissipation), which correlates to low thermal noise levels as can be seen in the above equation[1]. The monolithic stage consists of fused silica fibers connecting the penultimate mass to the ultimate mass/test mass/optic, as can be seen in figure 1.

Fused silica "ears" provide structural connection between the silica fibers and the silica test mass, and can also be seen in figure 1. The ears currently in use meet a set of basic criteria laid out for aLIGO: that the design includes attachment points for laser welding to the fibers, that the ears connect the the test mass to the fibers strongly with a minimum safety factor of 3, that the ear bond shear stress shouldn't exceed GEO600's maximum

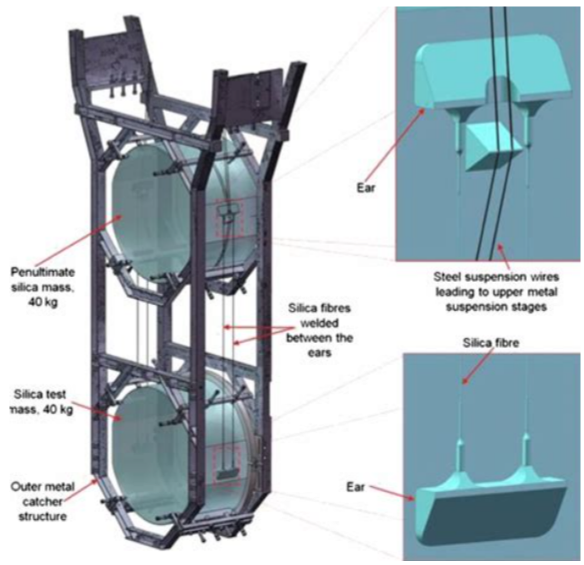

FIG. 1. aLIGO's Monolithic Fused Silica Final Stage [1]

value (0.16 MPa), that the bond won't degrade during welding because of high temperatures, and that the ears and their attachment bonds don't affect the thermal noise levels of a single test mass by more than 7 x 10^{-22} m $\mathrm{Hz}^{\frac{1}{2}}$ at 100Hz[1].

Though many of these requirements will still hold, It's possible that in future detectors larger test masses will require some re-engineering of these ears.

II. EAR MODELING

SolidWorks Professional 2021[12] was used to draw up the three-demensional geometries of various potential ear designs.

FIG. 2. GEO600 Dual Ears [7]

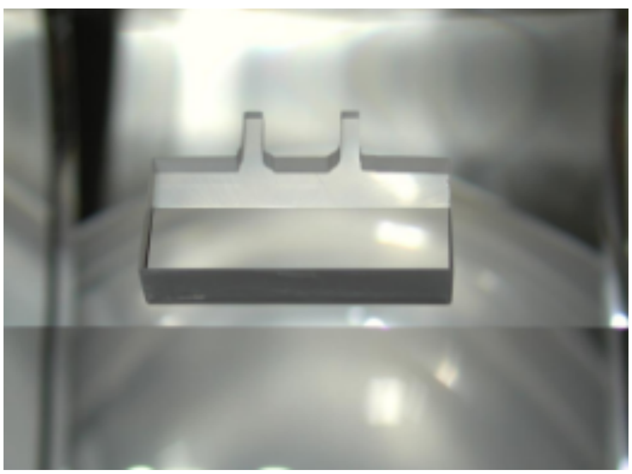

FIG. 3. GEO600 Final Ear Design [7]

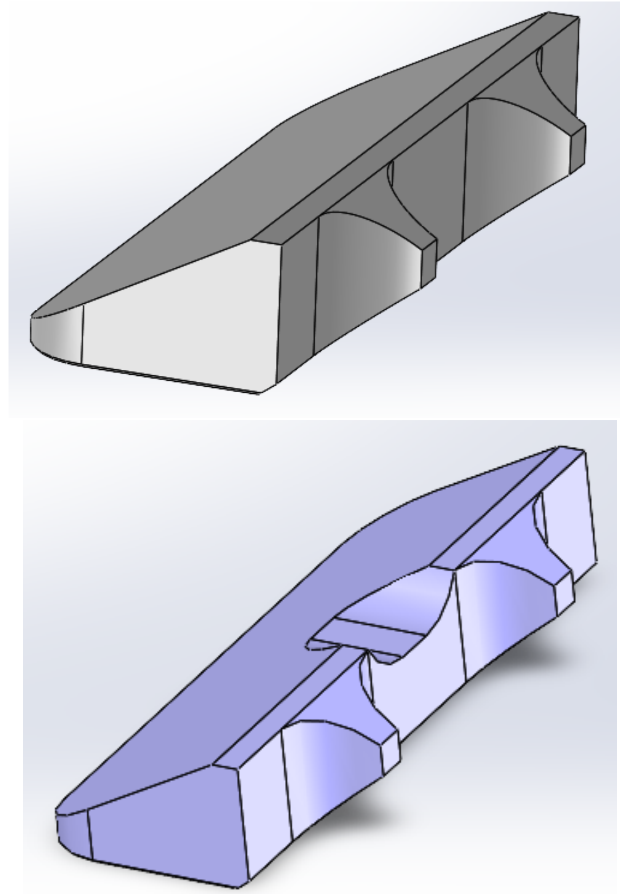

FIG. 4. Current aLIGO Ears

FIG. 5. 3D-Printed aLIGO Ear Prototype

A. Basis Ear Design

The finalized ear designs used for the monolithic final stage of Advanced LIGO's quadruple suspension were the basis for the adjusted models analyzed in this paper.

All of the work done in ear design analysis for this project was based upon functional designs that already existed. The first GEO 600 ears from the late 90s pioneered rectangular duo horns welded to circular fibers (see figure 2), and became the basis for later revisions resulting in GEO600's final one-piece ear design with more developed surface contours and body shapes.(see figure 3 [7]

aLIGO ears used a conceptually similar, but significantly enlarged design comprised of a main wedge with two horns attached for welding to the circular silica fibers. Note that there are two versions of the ear (see figure 4): one with a recess on top to keep from interfering with the steel wires that suspend the penultimate mass in the quadruple suspension. Figure 5 shows a life-sized 3D-printed ear prototype. This final design is currently used

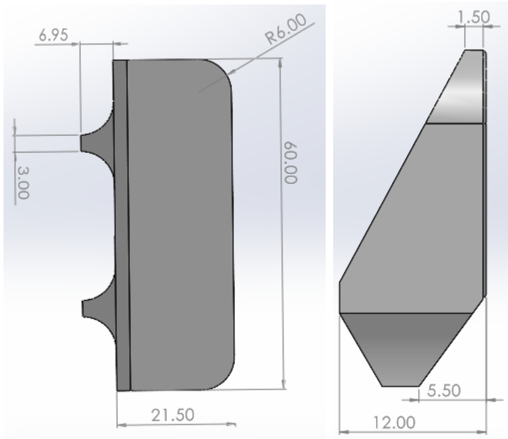

FIG. 6. Current aLIGO Ear Measurements (mm)

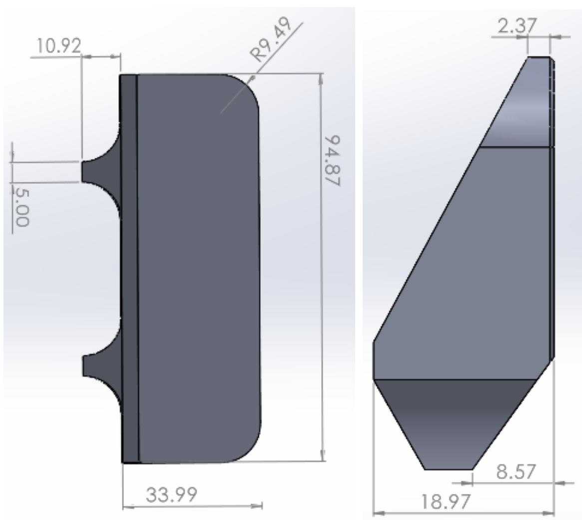

FIG. 7. Scaled-Up Ear for 05+ Measurements (mm)

in the final stages of aLIGO's quadruple suspensions, and was the basis for scaling and modeling adjustments done in this project. Exact measurements of the ear can be seen in figure 6, while figure 7 shows measurements on the scaled-up basis ear used for this project.

B. Important Ear Parameters

This subsection introduces the important variable ear parameters analyzed further in the paper.

The first of these is what we call wedge angle. This refers to the angle between the flat base of the ear and the sloped upper face of the ear. A higher wedge angle would mean a steeper slope and require more mass, while a lower wedge angle would be flatter. Both extremes can be seen in figure 8. Note that in analysis for this parameter, as wedge angle was increased, the top flat face on the ear was extended so that the height of the ear wouldn't change. This can also be seen in figure 8.

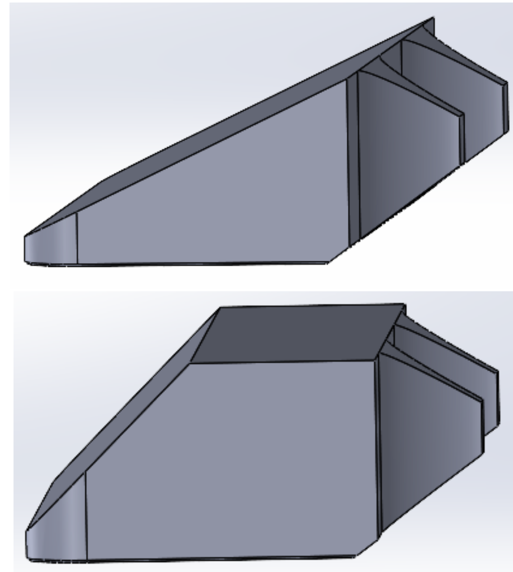

FIG. 8. Wedge Angle Visual

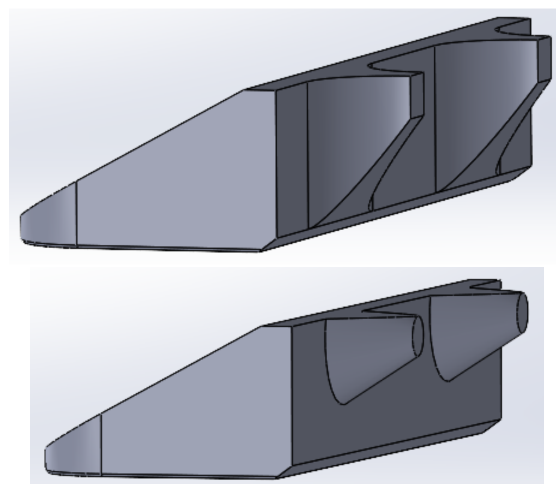

FIG. 9. Horn Position Visual

The second parameter needing definition is horn position. The horns of the ear are the two protrusions on the front face that weld to the silica fibers, and horn position refers to where the center axis of a horn is placed relative to the top and bottom of the front face of the ear. Chamfers on the horns are adjusted accordingly to match the new horn position. Figure 9 shows how ears look with horns placed at the top of the front face, in rectangular and conical horn cases. Conical horns can be cut to accommodate for the change in position, as seen here.

The third important parameter is something named 'front face height'. This actually refers to three variables coupled together purposefully, since changing them all at once makes for an intuitive way to heighten the ear. Increasing the front face height means making the ear

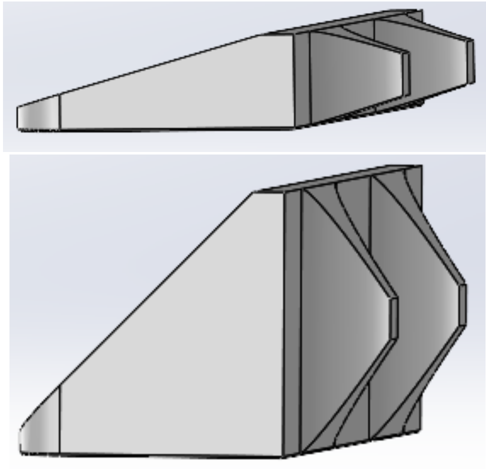

FIG. 10. Front Face Height Visual

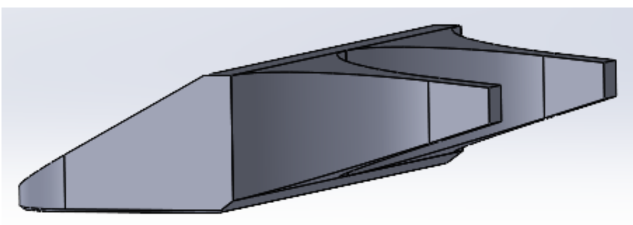

FIG. 11. Horn Length Visual

taller (front face becomes taller), increasing the wedge angle without changing the size of the flat face on top, and keeping the horns centered relative to the front face (which moves them up with the heightening of the front face). Figure 10 shows low vs high front face height.

One other parameter tested for this project was horn length. For larger horn lengths, the tip of the horn was extruded further from the ear and chamfers/fillets were adjusted accordingly. Figure 11 shows an ear model with 30 mm horns, which were the longest tested.

C. Subtleties to the Scaled-Up Ear

The current Advanced LIGO ears outlined above were scaled up from the GEO600 final ears such that the nominal bond shear stress was conserved with the increase in optic mass[4], where nominal shear stress

$$\tau_{ears} = \frac{mg}{nA}$$

and

g = gravitational constant ($9.81\ m * s^{-2}$)
m = test mass (kg)
n = number of ears per mass
A = bond surface area (m^2)

The aLIGO basis ear SolidWorks file was similarly scaled up for this project so that nominal shear stress

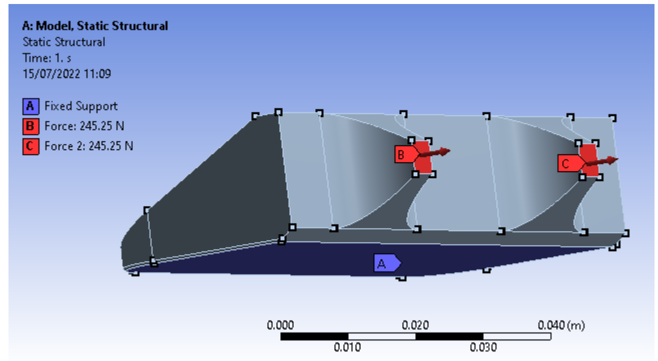

FIG. 12. Load Set on Ears

would be conserved. The projected optical test mass increase for the United State's next upgrade (05+) to aLIGO is from the current 40 kg up to 100 kg, or a factor of $\frac{100}{40} = 2.5$. To keep nominal shear stress at the same value, bond surface area A then had to be scaled up by a factor of 2.5. The entire model was scaled up in SolidWorks by a factor of $\sqrt{2.5} \approx 1.58$ to accomplish this.

However, one adjustment was made from the directly scaled-up version: the horns still had to be sized so that the weld area (square tips of the horns) would fit the silica fiber sizing intended for use in the 05+ upgrade. Currently, the plan is to pull those larger fibers from 5 mm diameter Suprasil 2 stock, as opposed to the 3 mm diameter stock used to pull current aLIGO fibers. The horn laser weld area was appropriately adjusted to be a 5 mm by 5 mm square (5 mm diameter circle for conical horn models), and the complete resized ear model is laid out in figure 7 (measurements in mm).

III. EAR PARAMETER ANALYSES

This summer project involved taking the basic 05+ scaled ear design outlined in section II and investigating the effects that changing specific parameters had on stress distributions in the ear. Each adjusted version was uploaded into ANSYS Workbench 18.1[6] to undergo static structural Finite Element Analysis testing the theories we had on what could improve or worsen stresses in the ear. Specifically, we checked effects on maximum principal stress throughout the volume of the ear, normal stress in the bond area, and shear stress in the bond area.

Finite Element Analysis (FEA) approximates solutions to continuous boundary-condition problems across a surface or volume by breaking that surface or volume into discrete "elements". These elements can be cubic or tetrahedral, with "nodes" at corners or edges. Problem values are solved at nodes, and the continuous solution distribution is then extrapolated from the discrete number of solution values already obtained.[8]

The structural analysis load settings applied to each of

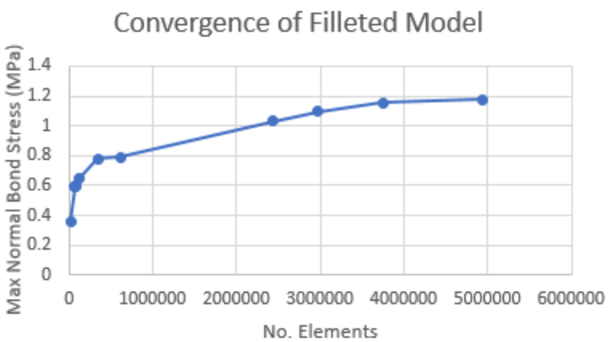

FIG. 13. Notably Smooth Convergence Chart

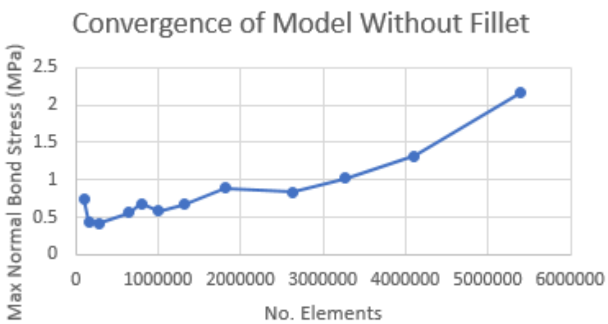

FIG. 14. Convergence Chart from model with Stress Singularity

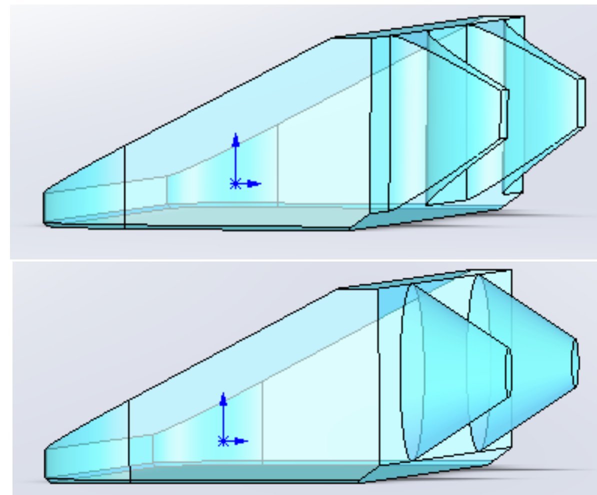

FIG. 15. Rectangular and Conical Horns

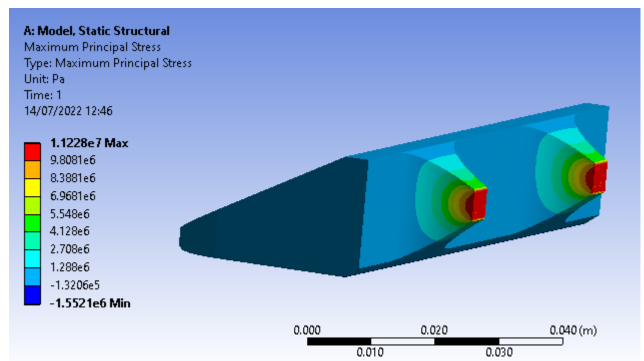

FIG. 16. FEA: Principal Stress Distribution on Basis Ear

the ears in the following section can be seen applied to the basis ear in figure 12. A fixed support is added to the base to replicate the ear's bond to the test mass, and a tensile force is applied normally to each horn weld face to represent the pull of the silica fibers on the ear.This force is calculated as follows: the test mass (100 kg) divided by 4 fibers per test mass (25 kg) times 9.81 $m*s^{-2} = 245.25$ N.

Since FEA is an approximation, special care had to be taken to make sure we were seeing accurate solutions. A model with a mesh-independent solution is desired, so convergence tests were run with varying mesh sizes (and therefore varying element size and number) to confirm an appropriate mesh size. With an appropriate mesh sizing, results can be very accurate without wasting too much time computing an unnecessarily high number of solution values. All of the analyses in this project were run at mesh values found through convergence tests.

Figure 13 demonstrates the smooth curve that converges to a single value in a successful convergence test. Mesh size should be chosen around the point where the curve stabilizes.

Figure 14 demonstrates what happens in the convergence test when the model has an undesired stress singularity. Stress singularities occur in the mesh where the stress value is theoretically infinite - this can happen when dealing with a point load, sharp corner, etc. If a stress singularity isn't noticed and dealt with, FEA results can be misleading as the maximum stress value won't stop increasing with mesh resolution. Sharp edge (or corner) stress singularities can be dealt with easily by adding a small fillet radius to the edge, which removes the point of theoretically infinite stress. This was done to the front base edge of the models in this project (0.1 mm fillet radius was used) so that stresses in the base surface could be analyzed accurately.

This section is sorted by parameter under analysis.

A. Horn Shape

The "horns" of the ear are the two protrusions that facilitate easier attachment of the silica fibres via CO_2 laser welding. The laser beam is reflected around the weld site to heat as evenly as possible. Changing from rectangular filleted horns to conical horns has been considered, but never yet implemented. There are a couple reasons that could explain this, the most likely being that the difference in shape doesn't affect stress distributions drastically, and rectangular horns have been used since

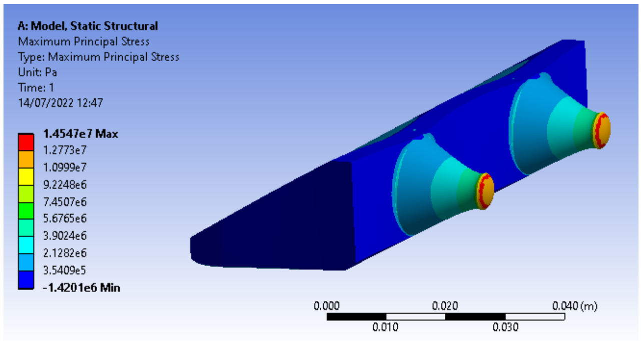

FIG. 17. FEA: Principal Stress Distribution on Conical Ear

GEO600. It's also much more practical to offset a rectangular horn than a conical one, since chamfers and fillets can be easily adjusted for asymmetry (observe these differences in figure 15). Since conical ears are by nature symmetrical, they may only be a viable choice to use in a case where the horns are positioned equidistant from the top and bottom of the ear's front face. However, the possibility of cutting the cone off to displace conical horns is explored in subsection C.

This being said, there are arguments to be made for the superiority of conical horns. The silica fibers welded to the horns are cylindrical, so having a circular weld site can simplify alignment during welding and of course provides a perfect fit to the fiber (whereas the square corners must be smoothed during welding). From a manufacturing standpoint, conical horns may also be simpler and cheaper to have made.

Note that figure 16 shows a maximum stress of 11.2 MPa in the untouched, scaled-up ear (described in section II). This maximum value acts as a comparison point for all of the design iterations for the 05+ ears. In this case, we compare it to the maximum stress observed in figure 17 (14.5 MPa) to note that, though stresses clearly get higher in the conical case, the maximum principal stress only increases by around 3 MPa from the rectangular case. As long as this increase is acceptable, conical horns remain a viable option for future ears.

This FEA was run on a mesh of about 600,000 elements.

B. Wedge Angle

When the test mass, ear size, and fiber stock size are all enlarged for 05+, some of the assembly procedures and methods may need to change to account for the increase in mass being dealt with. One such method may be heat distribution method for the CO2 laser weld that attaches the fibers to the ears[3]. Currently, a gold-plated angled mirror is slid between the horn and the mass, and the hot beam is carefully both applied directly to the outer side of the weld site and reflected to hit the inner side. With a 3 mm diameter weld site, this has been sufficient

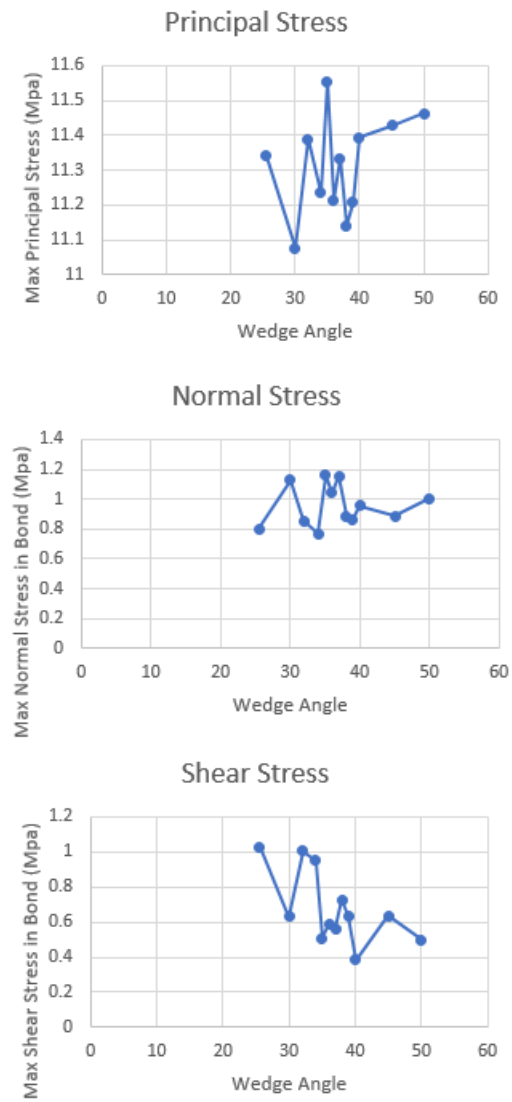

FIG. 18. Wedge Angle Stress Analysis Results

to evenly heat the circumference. However, hitting with heat from 2 sides may not be an even enough heating distribution to provide a desirable weld to future 5 mm diameter weld sites.

Taking this into account, an angled conical mirror is the current idea for evenly heating a larger weld site, this being derived from the method already successfully used to pull the fibers. A 3D-printed mock-up of this mirror design (about 10 cm across) can be seen around a silica "horn" in figure 22. This would focus the beam's heat all around the circumference. The only issue is that this mirror will require more open space between the horns and the test mass that we're used to. Taking this into account, one of the most important parts of this project was investigating how we could move the horns further away from the test mass in new ears without badly affecting stress distributions or manufacturability. This subsec-

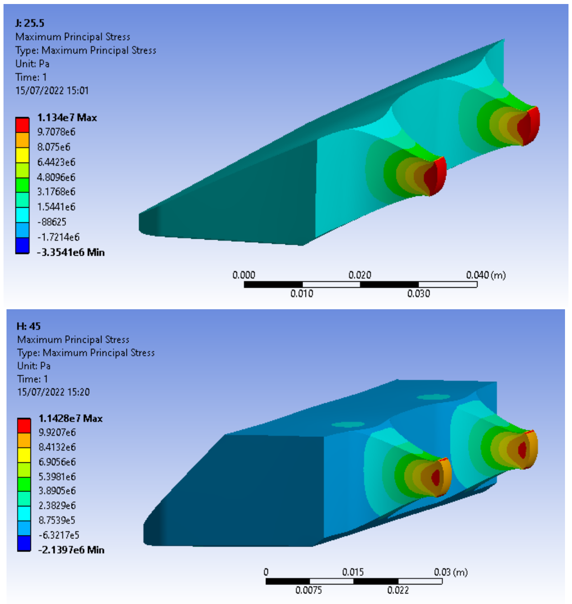

FIG. 19. FEA: Principal Stress Distributions

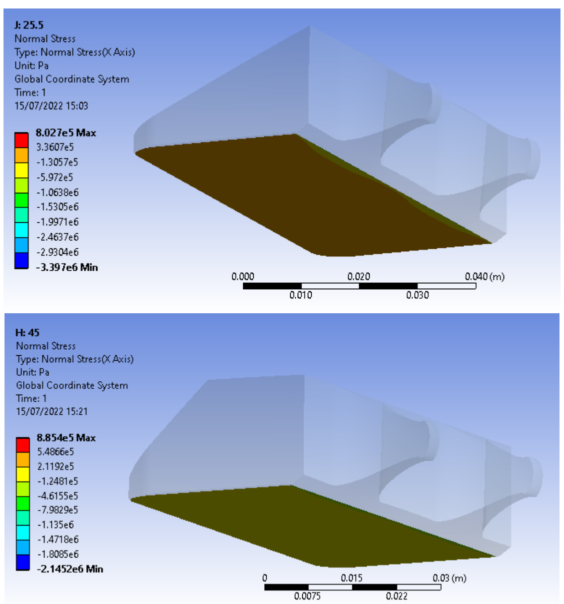

FIG. 20. FEA: Normal Bond Stress Distributions

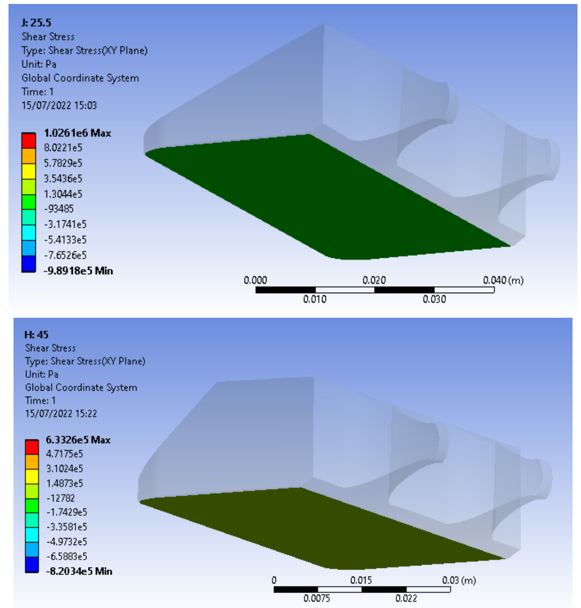

FIG. 21. FEA: Shear Bond Stress Distributions

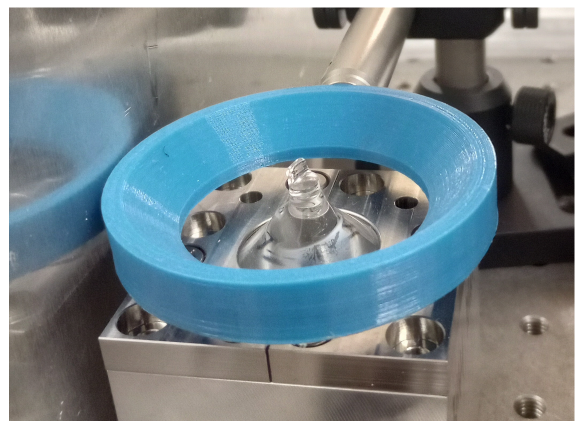

FIG. 22. Angled Conical Mirror Model

tion as well as subsections C, D, and E look at possible remedies to this problem.

One of the potential ways to increase distance between the weld faces and the test mass is to increase the wedge angle of the ear and subsequently lengthen the front face.

We ran ANSYS FEA over a range of wedge angles from 25 to 50 degrees testing the effect that angle alone would have on stress distribution. It's important to note that for the analysis, the angle was changed without lengthening the front face, since coupling those two variables was not desired for the testing of angle alone. Instead, the flat top face of the ear was lengthened as needed to make up for the steeper angle. See figures 19, 20, and 21 for FEA stress distributions of ears with wedge angles of 25.5 degrees and 45 degrees.

We also introduce a couple of new stress parameters for this analysis as well as the analyses in subsections C, D, and E. Since the driving factor for these particular analyses is getting the horns further away from the base of the ear, the force from the pull of the fibers may start to create more of a moment on the base of the ear.Observing the stress distributions on the base area of the ear, where the bond to the test mass is located, is therefore important in these analyses. We want these bond area stress distributions to stay fairly even, as some sort of 'peeling' torque could happen (when the fibers are moved further from the base) that threatens the integrity of, say, the delicate rear edge of the ear.

As can be seen from the results displayed in figure 18, there doesn't immediately seem to be much of a correlation between wedge angle and principal stress distribution. The only thing of note from that analysis run is that principal stresses appear to rise after 40 degrees, so perhaps a practical choice is to keep the wedge angle below 40 degrees. That being said, there's much uncertainty in that statement since the correlation is already so noisy and small to begin with.

There is no clear relationship between wedge angle and normal stress in the bond area (again see figure 18).

Interestingly, shear stress in the bond area seems to decrease with steeper wedge angles (figure 18). This is notably a good thing, and the same event can be observed in subsection D.

The wedge angle analysis was done using a mesh of about 4.5 million elements.

C. Horn Position

One of the most obvious ways to increase distance between the horn weld faces and the test mass is to move the center axes of the horns up to a higher position on the front face of the ear, making the horns more asymmetrical. The effects of this adjustment on stress were tested for both rectangular and conical horns.

The FEA results of this analysis for rectangular horns can be seen in figure 23, run with about a 3.5 million element mesh resolution. The relationship between each stress and distance from top of horn to top of ear is clearly negative. Even though the horns were moved all the way to the top of the front face for the case of zero distance, none of the stresses increased significantly (less than 1 MPa). From these results, the horns can be moved up the front face if necessary for welding, but it must be kept in mind that all of the stresses will likely increase, and this should be considered for large moves of the horn from its nominal central position.

The FEA results of this analysis done for conical horns are shown in figure 24 (distance in mm), run with about a 3.5 million element mesh. All three types of stresses seem to increase slightly as the horns were positioned closer to the top of the ear. Results are similar to the patterns observed for rectangular horns above. No stresses increased further than 1 MPa from their values in centered position, so moving up conical horns for welding room is another viable option while sacrificing a bit of ear strength.

D. Front Face Height

We ran an additional analysis to look at what happens when the height of the front face of the ear is increased. This is maybe the most intuitive way to move the weld area further from the optic. However, it's important to note that this analysis naturally coupled together three variables: front face height, wedge angle, and horn position. While increasing front face height in the SolidWorks models, the wedge angle was also increased to keep

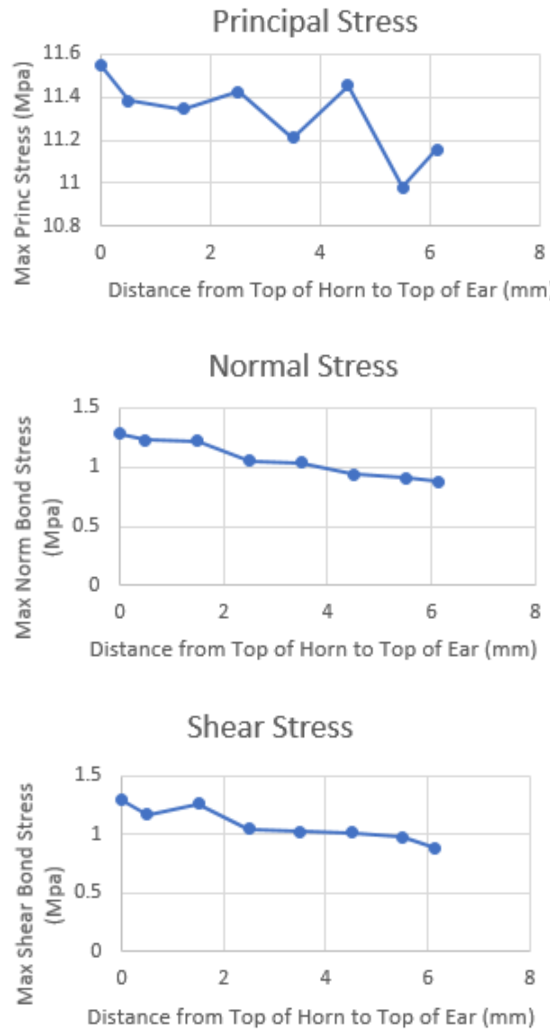

FIG. 23. Rectangular Horn Position Stress Analysis Results

from extending the entire ear to compensate. The horns were also kept centered (although their length was not altered), so they rose a bit with the center of the front face. Refer back to section II, subsection B to visualize this. This is a useful group to look at, since a solution coupling these three could likely occur in new ears to create welding space.

FEA results (run at about a 3 million element mesh resolution, which took about 30 minutes per model) for this analysis are shown in figure 25. Note that though the independent variable in these charts is 'wedge angle', these ears were drawn up uniquely with intentionally couple variables. As wedge angle increases, so does the height of the front face, and the distance between horns and ear base. So as the ears are made taller in this way, principal stress and normal stress (in base of ear) increase, while shear stress clearly seems to decrease the way it did in subsection B. Normal and shear stresses in the base stay quite low for the majority of this analy-

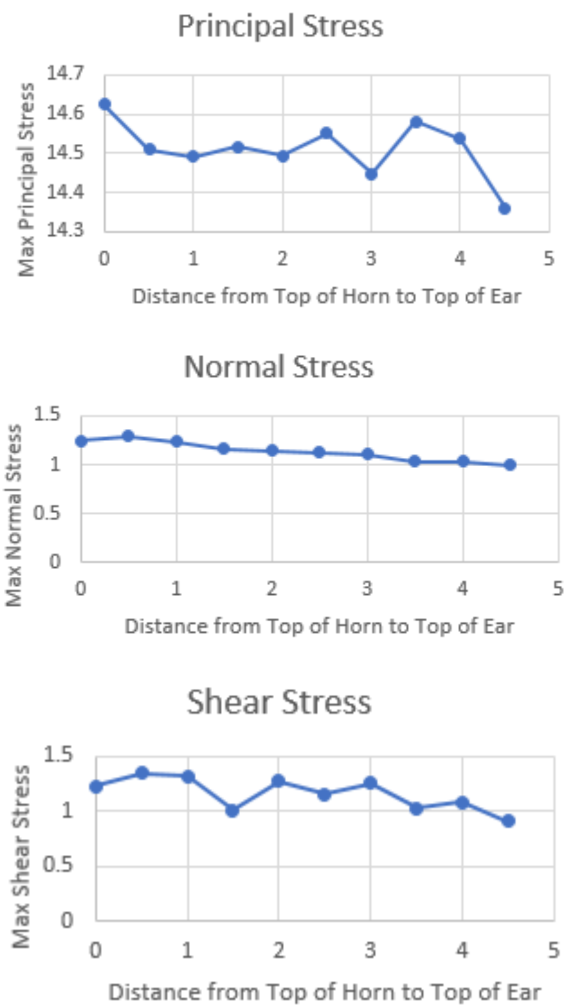

FIG. 24. Conical Horn Position Stress Analysis Results

sis, which is great. While keeping in mind that principal stresses will increase, this method of heightening the ear seems viable.

E. Horn Length

The last variable tested in the set of possibilities improving space for welding was horn length. Though extending the horns doesn't make for much extra distance between horns and test mass itself, this adjustment when combined with other design changes just gives more space for welding in general. Extra distance between the laser weld point and the nearest point of the bond on the ear base is likely to be necessary, as larger welds will deposit more power, and the bond needs to be kept under 400 deg C to avoid degradation[7]. The effect that horn length has on stress distributions in the ear could also just be useful to know about in case extending the horns is more practical for some future reason.

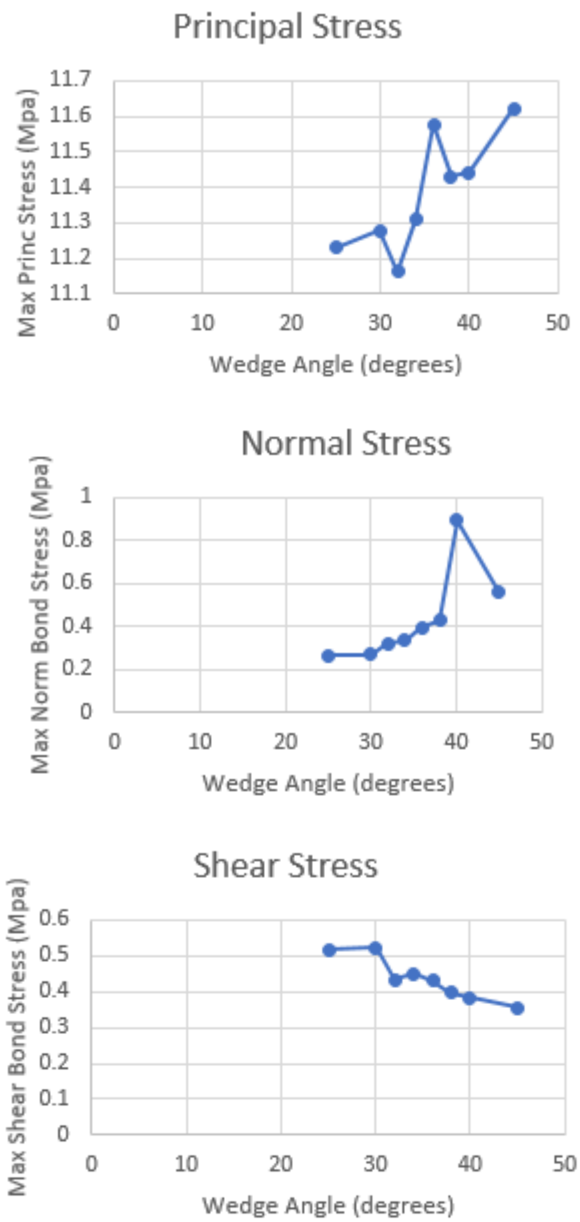

FIG. 25. Front Face Height Analysis

We weren't sure if this variable could affect stresses in the ears differently when the horns were placed at different heights, so we ran a horn length analysis with horns placed at each of three locations on the front face of the ear: centered (with respect to the base and top faces of the ear), top of horn flush with top of ear, and horn placed in the middle of these previous two. Figure 26 shows the basis model for each of these three placements.

All three of these separate FEA models were run at about a 3.5 million element mesh, and looked at horn lengths between 10 and 15 mm. For reference, the unadjusted, purely scaled-up horn length sits at about 9.5 mm, so this entire analysis was done with the purpose in

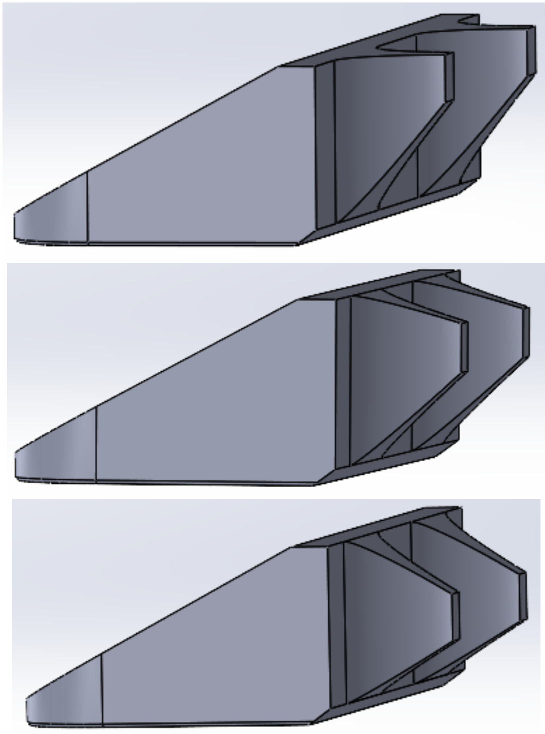

FIG. 26. 3 Basis Models for Horn Length Analysis

mind of increasing the length of the horns.

Figure 27 shows results for the centered horn. Only principal stress seems to be reliably affected by horn length at this placement; it clearly declines a bit with horns extended beyond about 15 mm. However, horn lengths between 10 and 15 mm don't seem to reliably affect stresses.

Figure 28 shows results for the horn placed in between top and center. Similarly, principal stress is inversely related to horn length at lengths above about 15 mm. Normal and shear stresses, once again, don't seem to be affected.

Figure 29 shows results for the horn flush with the top of the ear. Quite interestingly, principal stress increase once horn length is extended beyond around 20 mm at this placement in contrast to the decrease observed when the horns were placed further down on the front face of the ear.

It's valuable to know that, potentially, the length of the horns at any given height on the front face of the ear doesn't much affect normal or shear stresses throughout the ear. Principal stress, however, looks to be not only affected by horn length, but affected differently by the length at different placements on the front of the ear. This means that as long as the horns are kept low enough on the ear, they can be extended by quite a lot without negatively affecting stresses. However, if the horns are placed too high on the front face of the ear, care must be taken not to extend the horns beyond around 20 mm unless an increase in maximum principal stress in the ear is acceptable.

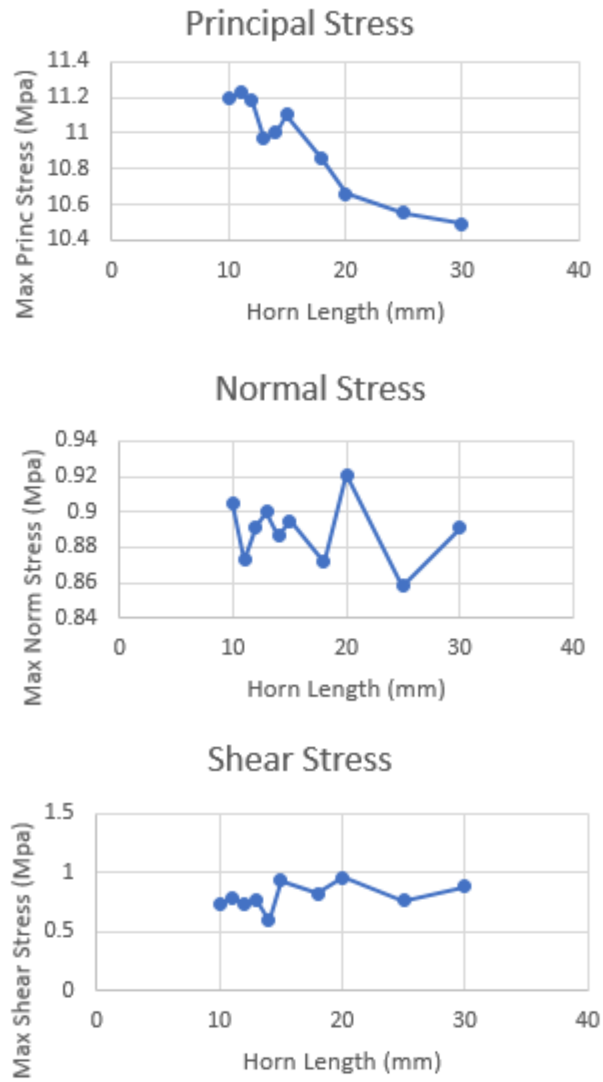

FIG. 27. Centered Horn Length Analysis

F. Miscellaneous

A few analyses were run just exploring observations made on the initial model. We wonder if certain details in the ear could be simplified without worsening principal stress distributions. All three of these analyses were done at about a 2 million element mesh resolution.

The first of these options explored was the possibility of taking away the tiny, .25 mm chamfer on the side, rear, and rear corner edges of the base of the ear. The ANSYS FEA resulting stress distribution of this adjustment can be seen in figure 30.The maximum principal stress in the ear with this design is about 11.6 MPa, compared to about 11.2 MPa max in the unadjusted design. Surpris-

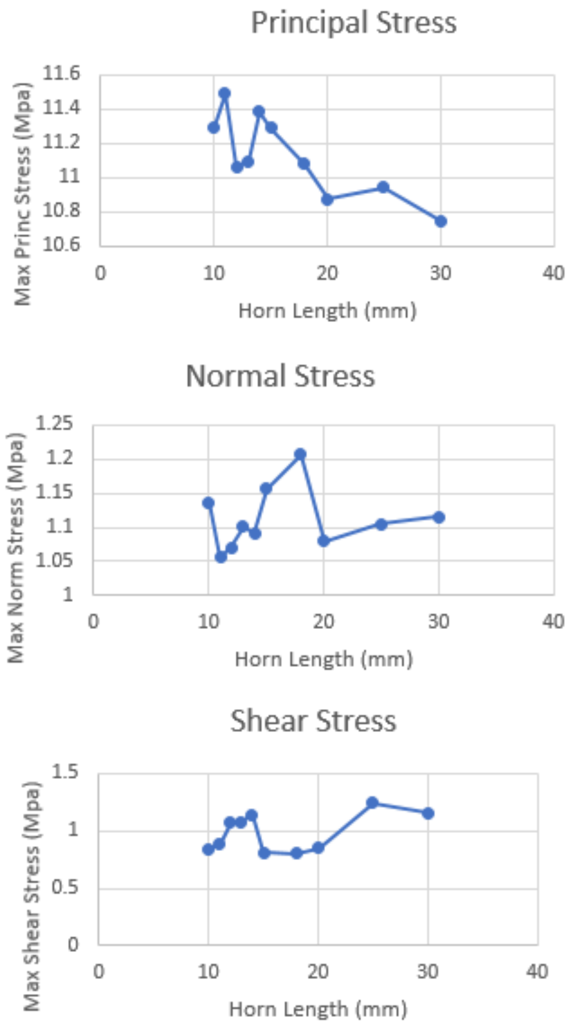

FIG. 28. Mid-placement Horn Length Analysis

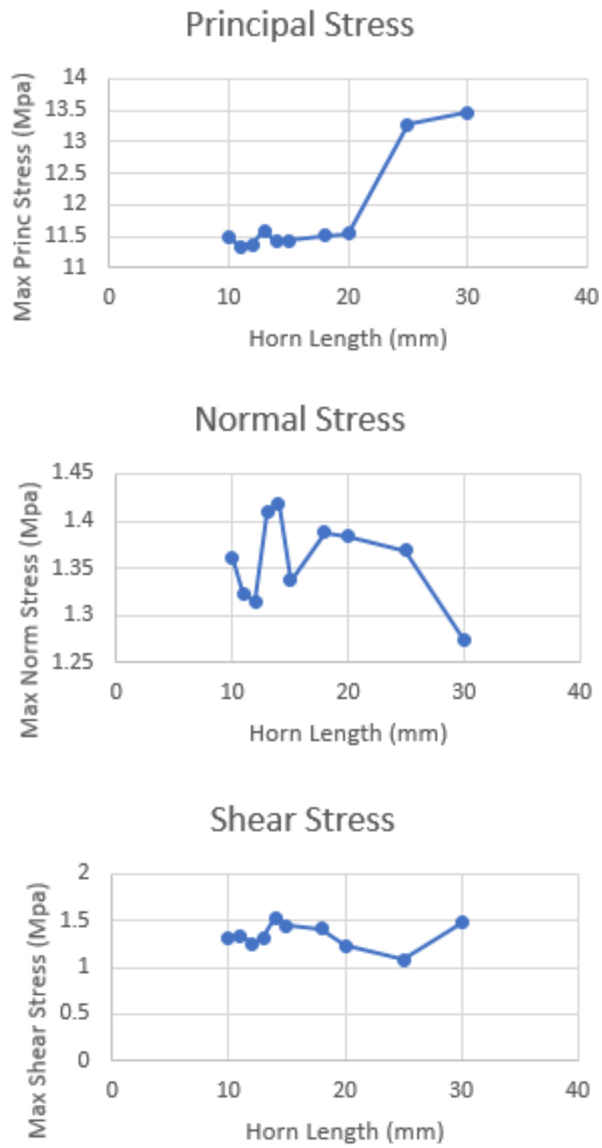

FIG. 29. Flush With Top Horn Length Analysis

ingly, maximum stress is lower with the base chamfer, so the best option seems to be to keep it.

The second adjustment made was taking away the 6 mm radius fillets on the two rear corners of the ear. Figure 31 shows the resulting FEA stress distribution in the new model. Once again, maximum stress was lower in the original ear model (11.2 MPa, compared to the new value of 11.4 MPa), so the rear corner fillets should be kept.

Lastly, out of curiosity, an ear was drawn up with rectangular horns that were chamfered all the way around instead of filleted on the sides. The stress distribution resulting from this adjustment can be observed in figure 32. With a maximum stress value of about 11.6 MPa, this is also an adjustment that increases stresses. The original horn design, with side fillets, should be kept as long as rectangular horns are still the shape of choice.

These analyses are useful to see, as they indicate that some of the features of the ears such as the base chamfers and rear fillets do serve some purpose in reducing

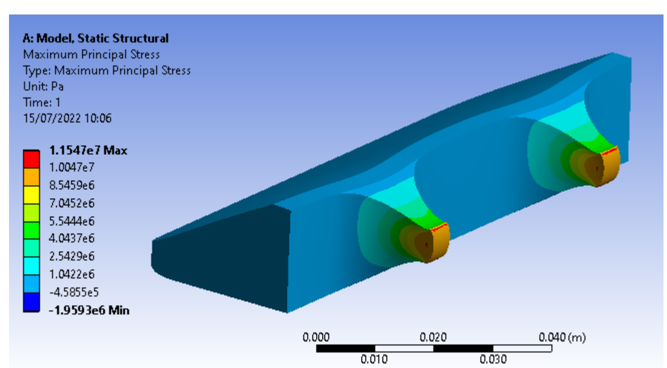

FIG. 30. FEA: Ear Without Base Chamfer

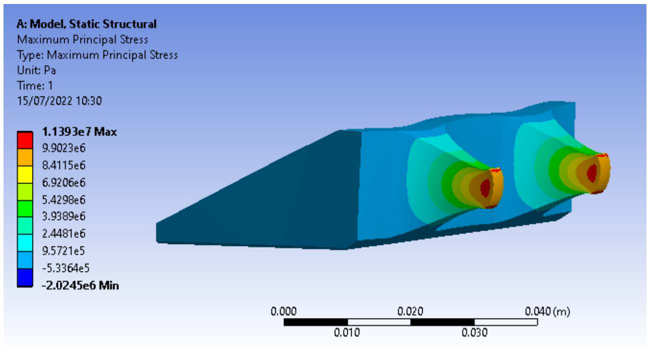

FIG. 31. FEA: Ear Without Rear Corner Fillets

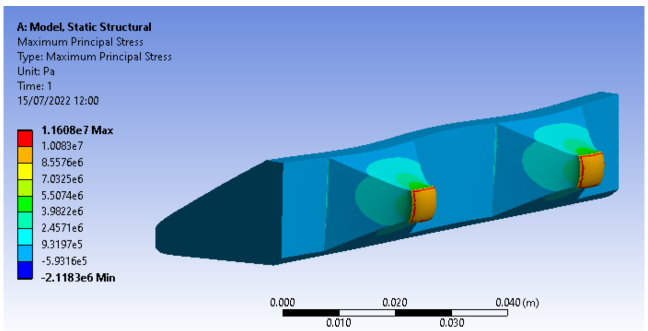

FIG. 32. FEA: Chamfered Horns

stresses. They also show that, if simplification of the ear design was desired without concern over small increases in stress, these features may not be needed.

IV. CONCLUSION

It's important to first note that this project only involved analyzing stresses in the ear, and we didn't additionally look at how adjusting the same parameters described throughout this paper would affect noise (thermal or other) in the ear or ear bond area. However, the effects of all of these adjustments on noise in the ear are crucial to look at, since keeping noise at a very low level is necessary for a successful gravitational interferometer. Future analysis should take a look at the noise distributions in some of the models created here that reduce stress.

With the disclaimer that, in this project, we only optimize stress distributions, there are a couple of potentially optimal ear redesigns that I propose. I offer two potential models, one each for the different possible horn shapes.

Firstly, if horn shape doesn't matter too much, I propose we stick with rectangular horns, since these can be made asymmetrical and can more easily provide an ear design that makes extra space for new weld mirrors. The top model in figure 33 conceptualizes my take on an ideal rectangular ear design with horns further away from the base, taking advantage of all the analyses run in this project. The wedge angle is increased to 38 degrees, and

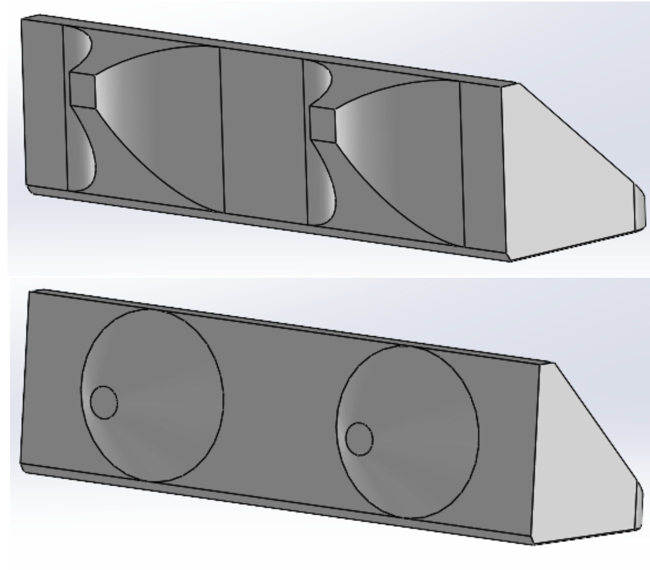

FIG. 33. Ear Redesigns

the front face is extended with the angle to 24.7 mm height (not including the front base chamfer). The horns are centered at about 20 mm up on this front face height, which is significantly skewed up from central position. The horns are also lengthened from the original 9.5 mm length to a new length of 13 mm, which additionally creates extra space around the weld area. This ear design gives 20.25 mm of space between the bond base of the ear and the center of the weld face on the horn.

If a switch from rectangular to conical horns is desired, a potential design is as in figure 33. This redesign incorporates a slightly taller ear and higher wedge angle to partially make up for the fact that conical horns must be centered on the front face. The bottom model (in figure 22) demonstrates this concept, with a wedge angle of 40 degrees and front face height of about 26 mm (again, not including height of the front base chamfer). Once again, in this model, horns are extended to a length of 13 mm, although this time they are of course positioned in the center of the front face of the ear. This ear design gives 14.7 mm of space between the bond base of the ear and the center of the horn weld faces, which is notably lower than the amount of space that the rectangular redesign gives. Subsection C explores the possibility of cutting the conical horns to allow change from central position, which removes the apparent limitation of going conical. Also note that the wedge angle could be further increased, or other parameters could be explored (such as lengthening the entire base of the ear to allow for a taller front without higher wedge angle) that would allow for more space around the weld.

ACKNOWLEDGMENTS

Primarily, I'm very thankful to the University of Florida International Research Experience for Undergraduates (IREU) program (especially Dr. Paul Fulda, Dr. Peter Wass, and Dr. Kathryn McGill) for selecting me for participation in this project abroad, paying me, arranging my flight/housing arrangements, and general problem prevention. I thank Nathanial Strauss, UF grad student, for being so helpful and organized with me and other IREU students. I also personally thank Dr. Alan Cumming and Prof. Giles Hammond, my mentors at the University of Glasgow, for their dedicated supervision and helpful direction regarding my summer research. Also, a big thanks to the many PhD students and post-docs in the University of Glasgow Institute for Gravitational Research who helped me in so many ways.

Lastly, I want to thank the National Science Foundation for funding my project, specifically under grant numbers 1460803 and 1950830.

REFERENCES

[1] A.V. Cumming et al. "Design and development of the advanced LIGO monolithic fused silica suspension". In: *IOPScience* 29 (2012).

[2] A.V. Cumming et al. "Large-Scale Monolithic Fused-Silica Mirror Suspension for Third-Generation Gravitational-Wave Detectors". In: *Physical Review Applied* 17 (2022).

[3] Hepstonstall A et al. "CO2 laser production of fused silica fibers for use in interferometric gravitational wave detector mirror suspensions". In: *Review of Scientific Instruments* 82.011301 (2011).

[4] M.van Veggel et al. "Final Design Document ETM/ITM Ears". In: *Advanced LIGO* 3 (2009).

[5] The LIGO Scientific Collaboration et al. "Advanced LIGO". In: *Classical and Quantum Gravity* 32.074001 (2015).

[6] *Ansys Mechanical Finite Element Analysis (FEA) Software for Structural Engineering*. URL: `https://www.ansys.com/products/structures/ansys-mechanical`.

[7] Alan Cumming. *Everything Ears (private communication)*.

[8] "Fundamental FEA Concepts and Applications". In: *ANSYS* ().

[9] Andri M. Gretarsson and Gregory M. Harry. "Dissipation of mechanical energy in fused silica fibers". In: *Review of Scientific Instruments* 70 (1999).

[10] Reid S Martin I. "Optical Coatings and Thermal Noise in Precision Measurements". In: *New York: Cambridge* (2012).

[11] Jim Hough Sheila Rowan Ginzton. "Gravitational Wave Detection by Interferometry (Ground and Space)". In: *Living Reviews in Relativity* 3.3 (2000).

[12] *SolidWorks 3D CAD*. URL: `https://www.solidworks.com/product/solidworks-3d-cad`.

[13] Kip S. Thorne Yuk Tung Liu. "Thermoelastic noise and homogeneous thermal noise in finite sized gravitational-wave test masses". In: *Physics Rev.* 62.122002 (2000).